Journal of Modern Physics, 2014, 5, 341-352
Published Online April 2014 in SciRes. http://www.scirp.org/journal/jmp
http://dx.doi.org/10.4236/jmp.2014.56044

Scientific Research

Analyses of $\pi^{\pm} - {}^{12}C$ Elastic Scattering and Reaction Cross-Section Data Below, Atop and Above the Δ-Resonance

Zuhair F. Shehadeh

Physics Department, Taif University, Taif, Saudi Arabia
Email: zfs07@hotmail.com

Received 10 January 2014; revised 11 February 2014; accepted 13 March 2014

Abstract

The pion-nucleus elastic scattering and reaction cross-section data at incident energies below, atop and above the Δ-resonance are analyzed using the full Klein-Gordon equation using an optical potential. Analytic forms of the potential are determined using the inverse scattering theory in those cases where phase shift analyses were available. The Coulomb effect is incorporated using Stricker's prescription. Both elastic scattering data and the reaction cross sections between 120 and 400 MeV are well reproduced. Both real and imaginary parts of the potential are local. The potential points determined by the inverse scattering theory in the interior region at 230 MeV clearly establish that the real part is repulsive. This remains the case at higher incident energies. The real part turns repulsive above the resonance, whereas the imaginary part reflects the dominance of surface absorption, which is maximum near atop the Δ-resonance and then falling off at higher energies.

Keywords

Pion-Nucleus Potential, Elastic Scattering, Inverse Scattering Theory, High Energy Physics

1. Introduction

Pions are key carriers of strong interaction among mesons and hadrons. Hence, the knowledge of pion-nucleon and pion-nucleus is an important starting point to gain insight into the physics of strong interaction. For this and general purpose of understanding mesonic physics, many research facilities around the world dedicated to meson physics such as Los Alamos Meson Physics Facility (LAMPF), Swiss Institute of Nuclear research/Paul-Sherrer Institute (SIN/PSI), Tri-University Meson Facility (TRIUMF), Brookhaven National Laboratory (BNL),

How to cite this paper: Shehadeh, Z.F. (2014) Analyses of $\pi^{\pm} - {}^{12}C$ Elastic Scattering and Reaction Cross-Section Data Below, Atop and Above the Δ-Resonance. *Journal of Modern Physics*, **5**, 341-352. http://dx.doi.org/10.4236/jmp.2014.56044

European Organization for Nuclear Research (CERN), National Laboratory for High Energy Physics (KEK), Joint Institute for Nuclear Research (JINR) and others were built in the late 20th century [1] [2].

Because of the very broad resonance associated with the Δ-excitation of a nucleon, it has been customary to categorize the elastic scattering of pions in three energy bins, namely incident energies up to about 100 MeV, noted as below the Δ-excitation, energies between 100 to 230 MeV, *i.e*. atop the broad Δ-resonance and energies greater than that, *i.e*. above the Δ-resonance [3]. The analyses reported in this paper cover the incident energies from 120 to 400 MeV. The kinetic energies being of the order of pion rest mass require a fully relativistic treatment to describe the reaction of the pions. Thus, this investigation is done using the full Klein-Gordon (K-G) equation unlike all previous ones which were usually done within the framework of an approximate version of K-G equation. The earliest works on pion-nucleus interaction were done using very limited data summarized in [4] [5]. The low-energy pion-nucleus elastic scattering data available at that time were primarily limited to forward angles and analyzed within the framework of non-local Kisslinger [6], local Laplacian [7] and local-equivalent of Kisslinger [8] potentials. All these theoretical models however, had only a limited success in explaining subsequent data taken at large angles. For explaining pion-nucleus scattering data in the delta resonance region at large angles, Satchler [9] proposed local potential similar to the one used in the optical model of nucleon-nucleus scattering using Schrödinger equation but considering relativistic kinematics (RSE). This paved the way for more pion-nucleus analyses using different local optical potentials [10]-[13] without recourse to the complexities of the non-local interaction. The successes of these potentials were reasonable but far from complete. In particular, all these analyses use RSE, which is an approximate form of the K-G equation.

Although Satchler's potential showed a remarkable success in analyzing pion-nucleus experimental data, it fails to account for large-angle pion-nucleus data when his potential was used in the exact K-G equation [14]. Shehadeh *et al*. [14] then used an inverse scattering theory (IST), suggested first by Hooshyar and Razavy [15] and developed by Alam and Malik [16] for non-relativistic cases and then by Shehadeh and Malik [17] for the K-G equation to determine the nature of the functional form of the potential. The Satchler potential determined using RSE had to be modified when used in conjunction with the K-G equation to account for large-angle pion-nucleus data. The nature of the pion-nucleus potential seems to be undergoing important functional change between 120 to 400 MeV incident pion energies. The real part of the potential seems to be monotonic and attractive below the delta resonance, turning to be non-monotonic atop the resonance and becoming repulsive above the resonance. Similarly, the nature of the absorptive part is dominated by surface absorption below and atop the resonance. A goal of this research is to ascertain these using the phase shift analyses available and doing a fit to the data using the K-G equation. This, to the best of our knowledge, has not been done. In fact, this research confirms these changes of pion-nucleus potential as one moves through the delta resonance. Furthermore, the data for 230 - 400 MeV reveal that pion real part of the potential is completely repulsive. The IST is based on extracting a number of points of the nuclear potential from available phase shifts using full Klein-Gordon equation for pion-nucleus systems. These extracted potential points are the most reliable in the exterior region, *i.e*. for $r > 2$ fm . The actual potential is then determined using these points as a guide. This potential, with its new analytical form, has been very successful in an analyzing pion-nucleus elastic scattering data in the low and delta resonance energy regions over the entire angles [18]-[20] for the elastic scattering of pions by ^{40}Ca. In addition, it has been successful in analyzing the data of elastically scattered charged pions from ^{54}Fe [21]. For charged pions, Coulomb effects are accounted for by implementing Stricker's prescription [22]. Relativistic kinematic and parameter values are calculated by following Satchler's treatment.

Although a variety of theoretical models have been used in the analyses of $\pi^{\pm}$-nucleus data above the delta resonance [23], only qualitative agreement between data and calculations was achieved [24]. In fact, in some cases, discrepancies between calculated elastic differential cross sections and data persist at forward angles; different models failed to account for the first diffraction minima in the measured elastic differential cross sections; and noticeable differences between calculations and data do exist at large angles. Most of the recent models used local optical potentials [25] [26] following Satchler's method. These potentials are used in a Shrödinger equation obtained by reducing a truncated Klein-Gordon equation, *i.e*. neglecting $V^2(r)/2E$ term, and redefining its kinematical quantities. Coulomb potential V_C was considered in its common form due to a uniformly charged sphere of radius R_C. Here, we'll follow Satchler's treatment, but with the inclusion of $V^2(r)/2E$ term, we use Stricker's prescription to substitute for V_C.

In addition to analyzing the elastic scattering data, we calculate the reaction cross section and compare it with data. This provides another check to the nature of absorption.

In the subsequent sections, theory, results and discussion, and conclusions are presented.

2. Theory

The IST used, as a guide, to extract the pion-carbon local optical potential, from available phase shifts and full K-G equation, is completely outlined in Ref. [18], and will not be repeated here. This extracted potential is then inserted into K-G equation for spinless relativistic cases. The non-monotonic nature of the real part of the potential is generated by having two potential functions. Similarly, to determine the interplay between volume and surface absorption, one needs at least two functional forms. Thus, the analytical form of the radial part of the potential is given by

$$V(r)=\frac{V_o}{1+\exp\left(\frac{r-R_o}{a_o}\right)}+\frac{V_1}{\left[1+\exp\left(\frac{r-R_1}{a_1}\right)\right]^2}+i\frac{W_2}{1+\exp\left(\frac{r-R_2}{a_2}\right)}+i\frac{W_3\exp\left(\frac{r-R_3}{a_3}\right)}{\left[1+\exp\left(\frac{r-R_3}{a_3}\right)\right]^2}, \tag{1}$$

For such a spherical symmetric potential, the radial part of K-G wave function, $R_{nl}(r)$, satisfies the following equation:

$$\left[\mathrm{d}^2/\mathrm{d}r^2+k^2-U(r)-\frac{l(l+1)}{r^2}\right]R_{nl}(r)=0, \tag{2}$$

where $R_{nl}(r)$ is the r times the radial part of the wave function for a spherical symmetric external potential. Also, in Equation (2), k^2 and $U(r)$ are given by

$$k^2=\left(E^2-m^2c^4\right)/\hbar^2c^2, \tag{3}$$

$$U(r)=\frac{2E}{\hbar^2c^2}\left[V(r)-V^2(r)/2E\right], \tag{4}$$

In Equation (3), E and m are the effective pion energy and effective pion mass, respectively, calculated by following Satchler's relativistic correction treatment as explained below, and c is the velocity of electro-magnetic wave in vacuum. $V(r)$ is the complex pion-nucleus potential. The Coulomb potential V_C is included as a constant according to Stricker's prescription and not as a function of r due to a uniformly charged sphere of radius R_C.

The elastic differential cross section is calculated by using the following relation:

$$\frac{\mathrm{d}\sigma}{\mathrm{d}\Omega}=\left|f(\theta)\right|^2, \tag{5}$$

with $f(\theta)$ is the total scattering amplitude at an angle θ in the center of mass system:

$$f(\theta)=f_c(\theta)+\frac{1}{2ik}\sum_{\ell=0}^{\infty}(2\ell+1)\exp(2i\sigma_\ell)\left[\exp(2i\delta_\ell)-1\right]P_\ell(\cos\theta), \tag{6}$$

where $f_c(\theta)$ is the point Coulomb scattering amplitude, σ_ℓ is the point Coulomb phase shift, δ_ℓ is the complex nuclear phase shift, and $P_\ell(\cos\theta)$ is the Legendre polynomial.

In many previous studies, the $V^2(r)/2E$ term in (4) was neglected. In our recent studies [14] [18], we showed that the inclusion of this term is important in accounting correctly for large-angle differential cross sections. The large angle data are particularly important in determining the uniqueness. The Coulomb part is considered by using Stricker's treatment. It is determined by changing the effective pion's incident energy by the Coulomb barrier height, which is ± 3.4 MeV in this case, calculated from the relation:

$$V_c=\pm\frac{Z_Te^2}{R_c}, \tag{7}$$

where $Z_T=6$ is the target's atomic number, $e^2=1.44\ \mathrm{MeV}\cdot\mathrm{fm}$, and $R_c=2.54$ fm is the effective Coulomb

radius. The negative and positive signs are for π^+ and π^-, respectively.

As a further test to the correctness of our potential, the reaction cross section σ_r was calculated using:

$$\sigma_r = \frac{\pi}{k^2}\sum_{\ell=0}^{\infty}(2\ell+1)\left[1-\left|S_\ell\right|^2\right], \tag{8}$$

where $S_\ell = \mathrm{e}^{2i\delta_\ell}$ is the S-matrix.

The kinetic energy, k^2, in Equation (2) is in the center of mass system, whereas the experimental kinetic energies, K_ℓ, are given in laboratory system. We use the Satchler prescription to transform K_ℓ to the center of mass as done in the most theoretical treatments. The method relies on transforming the true pion mass m_π and the pion bombarding energy in the laboratory system K_ℓ to the effective mass of the incident pion M_π and the actual beam energy $E_\ell = E_{c.m.}\left(M_\pi + m_T\right)/m_T$ where m_T is the target mass. Satchler's treatment, followed by several authors, is summarized as follows:

The center-of-mass kinetic energy, $E_{c.m.}$, is defined as

$$E_{c.m.} = \frac{\hbar^2 k^2}{2\mu}, \tag{9}$$

where $\hbar k$ is the relativistically correct center-of-mass momentum of the pion, and μ is the reduced mass of the two interacting particles:

$$\mu = \frac{M_\pi m_T}{M_\pi + m_T}, \tag{10}$$

where the effective mass of the incident pion M_π is defined as

$$M_\pi = \gamma_\pi m_\pi, \tag{11}$$

with $\gamma_\pi = \left(x+\gamma_\ell\right)\left(1+2x\gamma_\ell+x^2\right)^{-1/2}$ where $x = m_\pi/m_T$ and $\gamma_\ell = 1+K_\ell/m_\pi c^2$ with $m_\pi c^2 = 139.6$ MeV. In Equation (7), k is given by:

$$k = \left(\frac{m_\pi c}{\hbar}\right)\left(\gamma_\pi^2-1\right)^{1/2} = \frac{1}{m_\pi}\left(\frac{m_\pi c^2}{\hbar c}\right)m_\pi\left(\gamma_\pi^2-1\right)^{1/2} = \left(0.707587814\right)\left(\gamma_\pi^2-1\right)^{1/2}\ \mathrm{fm}^{-1}, \tag{12}$$

In atomic mass units u, one can use $m_\pi = 0.1499u$ and $m_T = 12u$ for ^{12}C. With this, one can rewrite Equation (9) as,

$$E_{c.m.} = 20.901\frac{k^2}{\mu(u)}\ \mathrm{MeV}, \tag{13}$$

Substituting Equations (10) and (12) in Equation (13), $E_{c.m.}$ can be easily calculated.

3. Results and Discussion

The success of our potential, in describing the elastic scattering of charged pions from calcium isotopes and ^{54}Fe at 180 MeV which lies in the delta resonance region of pions, forms a strong motivation for using its functional form to analyze pion-carbon elastic scattering data. This is because, so far, no potential has been capable of explaining $\pi^\pm - {}^{12}\mathrm{C}$ large angle data, and the nature of the real part of the potential has been long remained controversial [26]. We start by analyzing $\pi^\pm - {}^{12}\mathrm{C}$ elastic scattering data at 162 MeV where differential cross sections and phase shift analyses are available for both positive and negative pions. Our analyses establish that the non-Coulomb part for both $\pi^+ - {}^{12}\mathrm{C}$ and $\pi^- - {}^{12}\mathrm{C}$ is the same at this energy. Then, we extend the analysis to two nearby energies also atop the resonance region, namely 150 and 180 MeV. In addition, and to test the capability of our potential, we continued the analysis at energies below and above the delta resonance, namely 120, 200, 230, 260, 280 and 400 MeV. As pointed out in our recent work [20] [21], the parameters of our potential are modified so that both its real and imaginary parts match in the exterior region reasonably well, with the potential points obtained by the IST using available phase shifts and full K-G equation. These potential parameters,

used for describing the experimental data successfully, are presented in **Table 1**.

As noted earlier, we first analyze the data at 162 MeV, which is in the Δ-resonance region and the data for both $\pi^{\pm}$ elastic scattering are available. To fit both $\pi^{\pm}$ data at the same energy, with the same potential parameters, is an extra-constrain on the parameters search which determined our choice of the potential at this energy. We also provide the reaction cross-section data for both cases at this energy. Unfortunately no data are available.

Using the available phase shifts, we first determine the dotted points in **Figure 1** using IST. These points should be quite good to determine the exterior part of the potential e.g. potential at $r \geq 2$ fm . The parameters of the potential are then determined to reproduce the external points reasonably well. The final parameters set, noted in **Table 1**, is then obtained from fitting the differential cross section which, as shown in **Figure 1**, is very good. In particular, both minima are well reproduced. The calculated reaction cross sections, $\sigma_r(theor)$, shown in **Table 1** are in excellent agreement with the available data.

Next, we analyze the data for π^- scattering at 150 MeV for which the phase shift analysis is available. The data also extend to 150° *i.e.* there is some information on back angle scattering. The determined potential from IST as well as the fit to the differential cross section are shown in **Figure 2**. Both the fits to the differential cross section and the calculated reaction cross section, noted in **Table 1**, are very good.

Unfortunately at the three nearby energies, namely 120, 180 and 200 MeV, no phase shift analyses are available. As such, these data are analyzed using the potential parameters determined for 150 and 162 MeV as guides. The potential parameters used, along with reaction cross sections, are listed in **Table 1**. The corresponding potentials, real and imaginary parts, with calculated and measured differential cross sections are shown in **Figures 3-5** for 120, 180 and 200 MeV, respectively. In all these cases, the calculations reproduce quite well data at backward angles as well as the reaction cross sections. In particular, large-angle differential cross section data has been explained very well. To the best of our knowledge, no other potential has been successful in explaining these large-angle data.

Turning to the elastic scattering data on π^- at 230, 260 and 280 MeV, there is a sudden change in the pattern of the differential cross section – it seems that the second minimum gradually is disappearing with increasing energy and the cross sections fall off smoothly. Unfortunately, there are no data at large angles. This change

Table 1. The potential parameters used in Equation (1) for incident charged pions on ^{12}C target at energies T_π noted in column one. Our calculated reaction cross sections $\sigma_r(theor)$ in millibarns are compared with experimental values $\sigma_r(expt)$ in millibarns [26]. Data for both π^+ and π^- are available only for 162 and 400 MeV. The same parameters are used for $\pi^{\pm}$ at these two energies and hence are not shown for the π^- case.

T_π	V_o	R_o	a_o	V_1	R_1	a_1	W_2	R_2	a_2	W_3	R_3	a_3	$\sigma_r(theor)$	$\sigma_r(expt)$
(MeV)	**(MeV)**	**(fm)**	**(fm)**	**(MeV)**	**(fm)**	**(fm)**	**(MeV)**	**(fm)**	**(fm)**	**(MeV)**	**(fm)**	**(fm)**	**(mb)**	**(mb)**
$120(\pi^-)$	−24	2.20	0.474	−150	1.50	0.333	−10.0	2.30	0.766	−211.6	2.50	0.420	433	429 ± 18
$150(\pi^-)$	−25	3.00	0.474	−140	1.65	0.333	−10.0	2.30	0.766	−311.6	2.30	0.420	443	441 ± 18
$162(\pi^+)$	−25	3.00	0.474	−140	1.65	0.333	−10.0	2.30	0.766	−311.6	2.05	0.520	471	Not Available
$162(\pi^-)$													477	Not Available
$180(\pi^-)$	−37	3.00	0.474	−80	1.65	0.333	−10.0	2.30	0.766	−251.6	2.25	0.420	419	423 ± 13
$200(\pi^-)$	−20	3.00	0.474	−50	1.65	0.333	−25.0	2.30	0.766	−211.6	2.10	0.420	396	396 ± 13
$230(\pi^-)$	+65	2.40	0.474	−30	1.85	0.333	−22.0	2.50	0.766	−151.6	2.20	0.420	350	359 ± 18
$260(\pi^-)$	+26	3.00	0.474	+30	1.65	0.333	−15	2.30	0.766	−211.6	2.05	0.420	319	324 ± 19
$280(\pi^-)$	+26	3.00	0.474	+30	1.65	0.333	−15	2.30	0.766	−211.6	2.05	0.420	311	311 ± 19
$400(\pi^+)$	+20	2.75	o.474	+20	2.65	0.333	−45	2.30	0.476	−11.6	2.10	0.270	203	Not Available
$400(\pi^-)$													207	203 ± 11

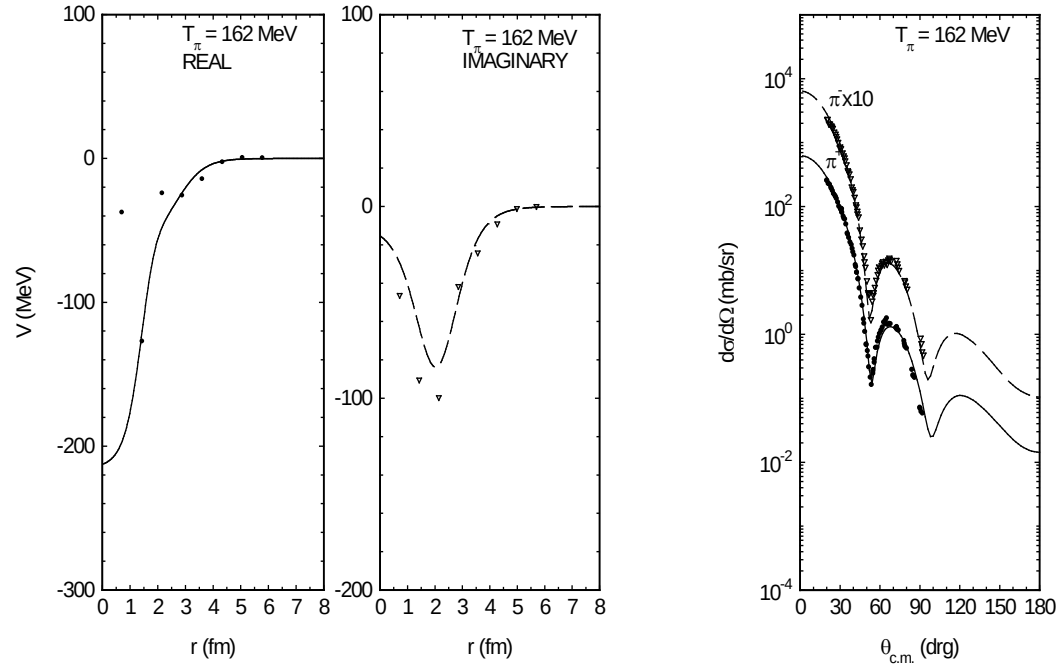

Figure 1. The left two figures indicate the analytical form of our potential, its real and imaginary parts as solid lines and compare them to the extracted potential points obtained using IST from available phase shifts [27]. The right most figure shows the excellent agreement between calculated and measured elastic differential cross sections [28], for $\pi^{\pm} - {}^{12}C$ at 162 MeV.

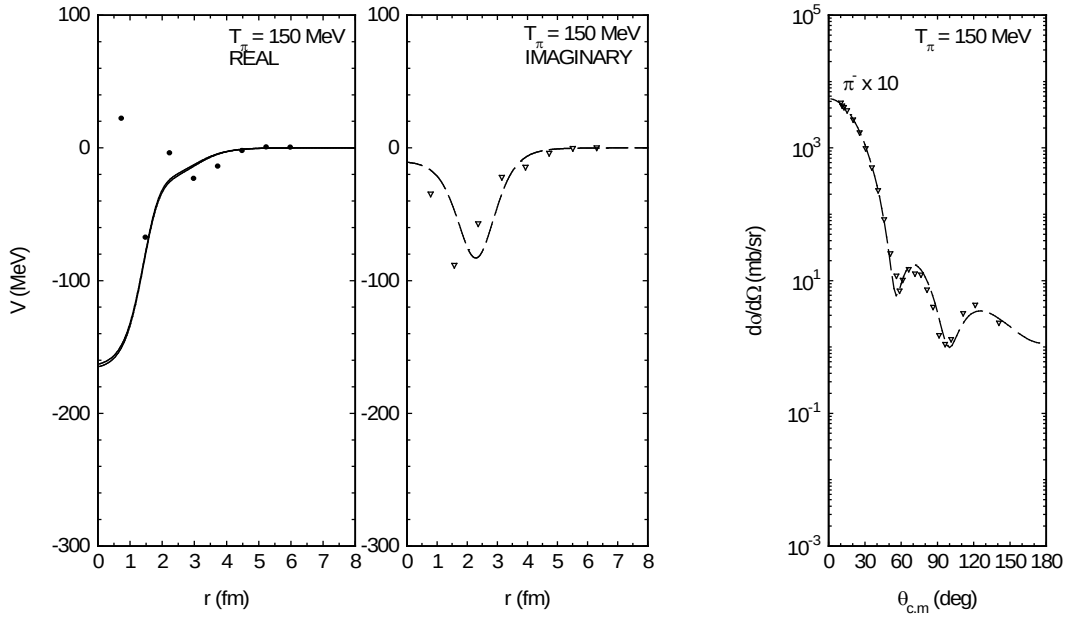

Figure 2. Same as **Figure 1** but for $\pi^- - {}^{12}C$ at 150 MeV. Data are from Binon *et al*. [29].

in pattern is reflected in the potential points determined using IST for 230 MeV incident energy shown in **Figure 6**. The real part of the potential in the interior is turning repulsive. This is a crucial result of the IST and leaves no possibility that the real part could be attractive. Also the repulsive nature of the real part is particularly pronounced at 260 and 280 MeV as shown in **Figure 7** and **Figure 8**. At all these energies, the calculated reaction cross sections are in excellent agreement with the observed ones.

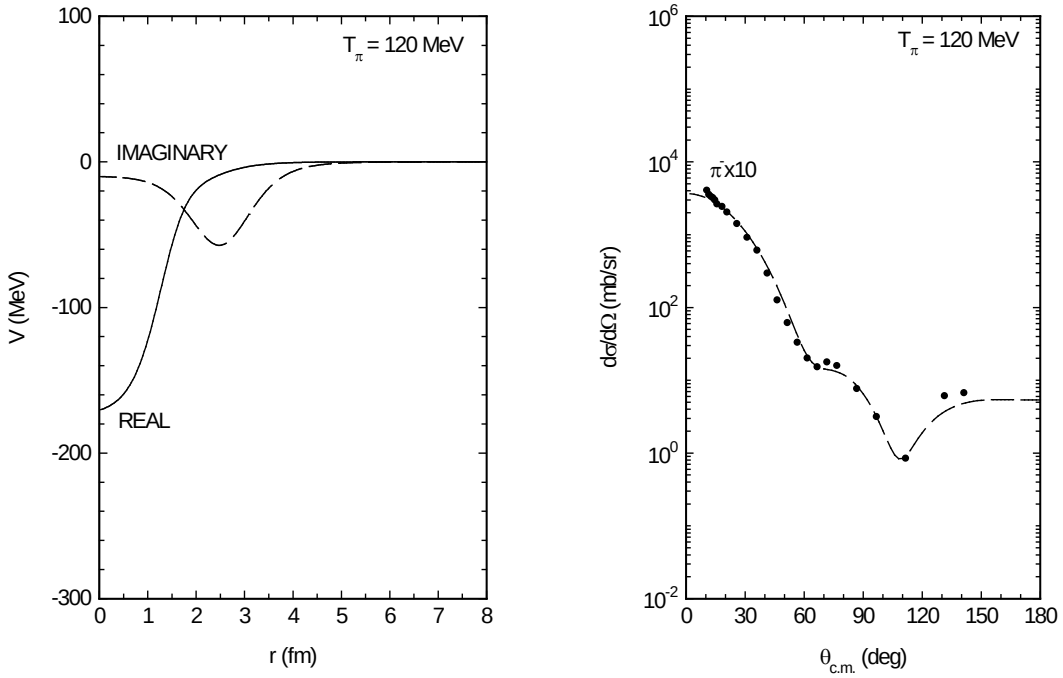

Figure 3. Same as **Figure 1** but for 120 MeV incident energy. No phase shift analysis is available and hence, there are no dots or empty triangles in the figure at left.

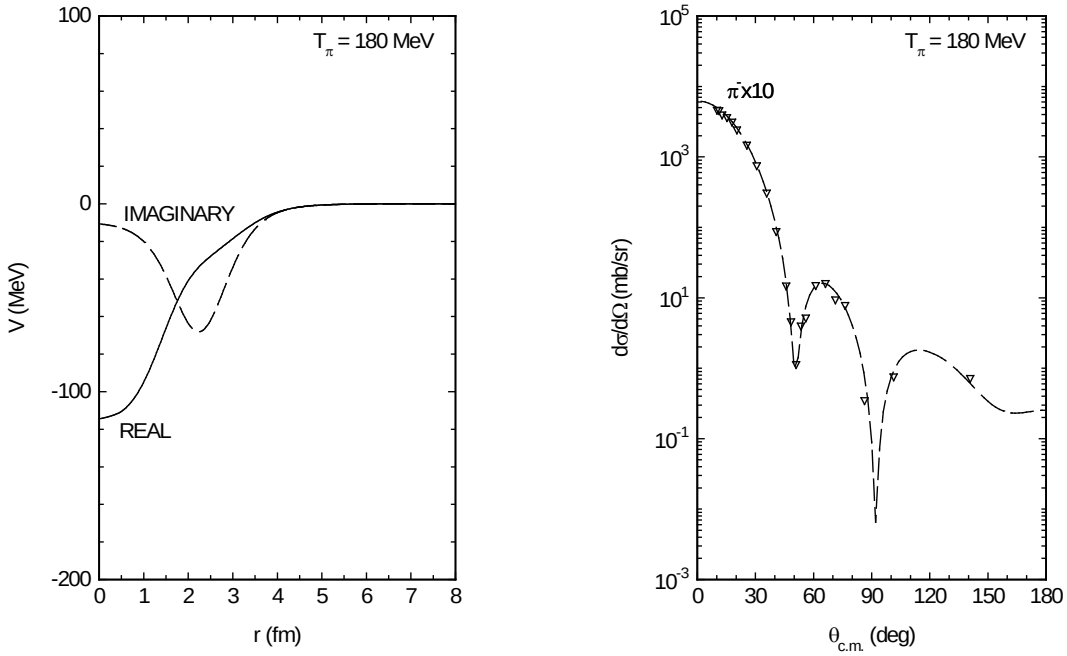

Figure 4. Same as **Figure 3** but for 180 MeV incident energy.

We particularly draw the attention to the IST-determined points in the region $r > 2$ fm . They clearly indicate the repulsive nature of the real part of the potential at 230 MeV. To examine further the nature of potential at higher energies, we fit the elastic differential cross sections at 260 and 280 MeV. As phase shift analyses are not available, we fit the data by adjusting the potential parameters used for the 230 MeV case. The potentials used, with their adjusted parameters shown in **Table 1**, have been very successful in explaining the elastic differential cross sections and in accounting for reaction cross sections. These potentials, with their real and imaginary

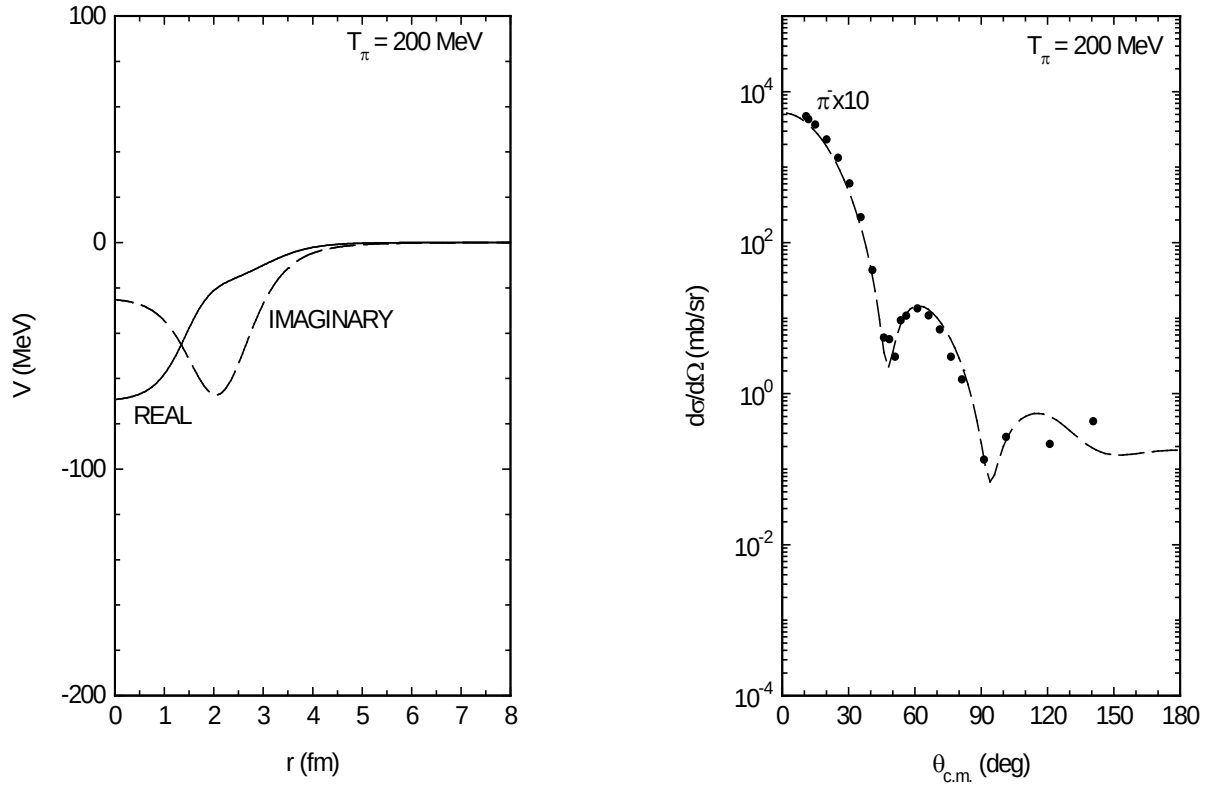

Figure 5. Same as **Figure 3** but for 200 MeV incident energy.

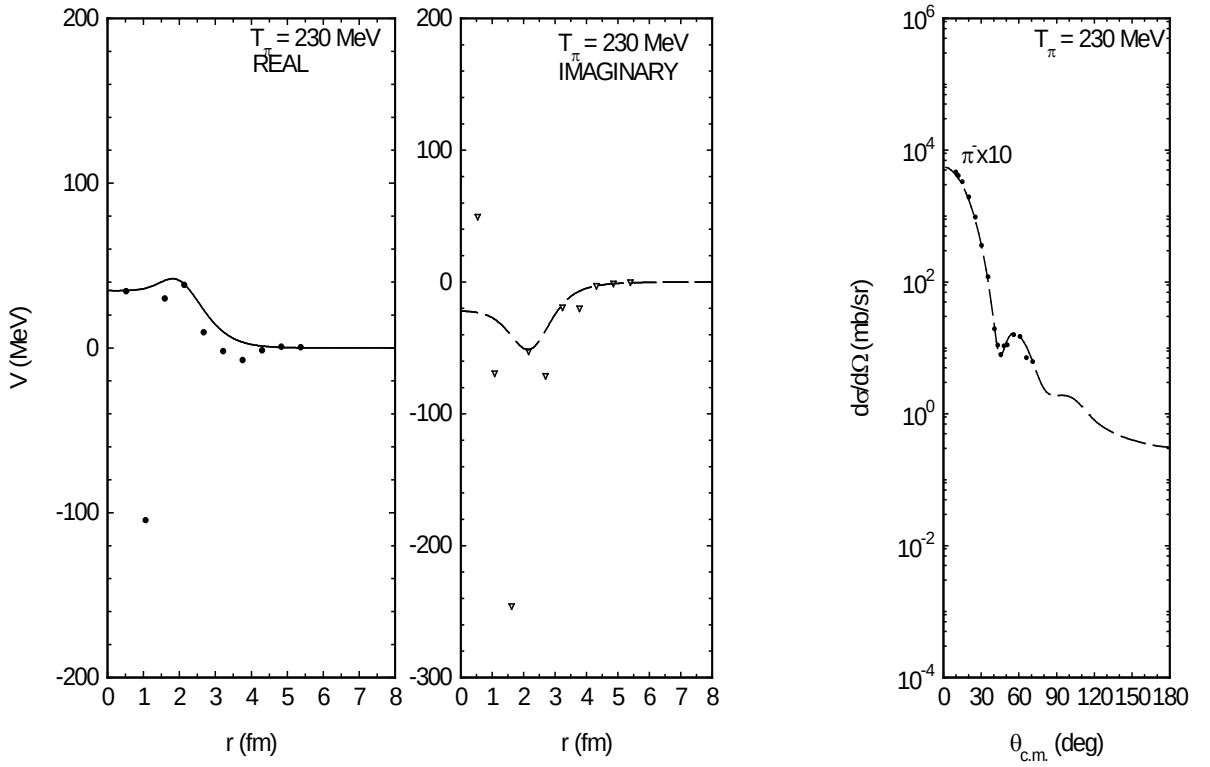

Figure 6. Same as **Figure 1** but for 230 MeV incident energy.

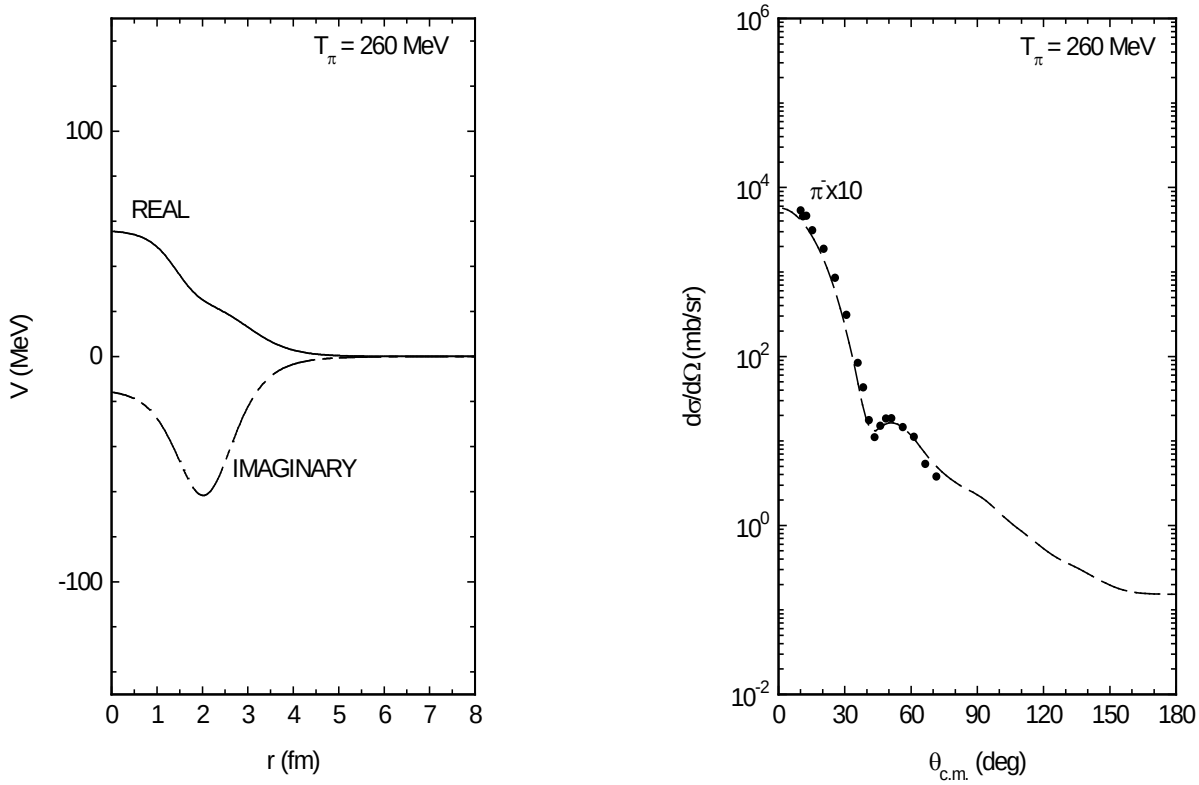

Figure 7. Same as **Figure 3** but for 260 MeV incident energy.

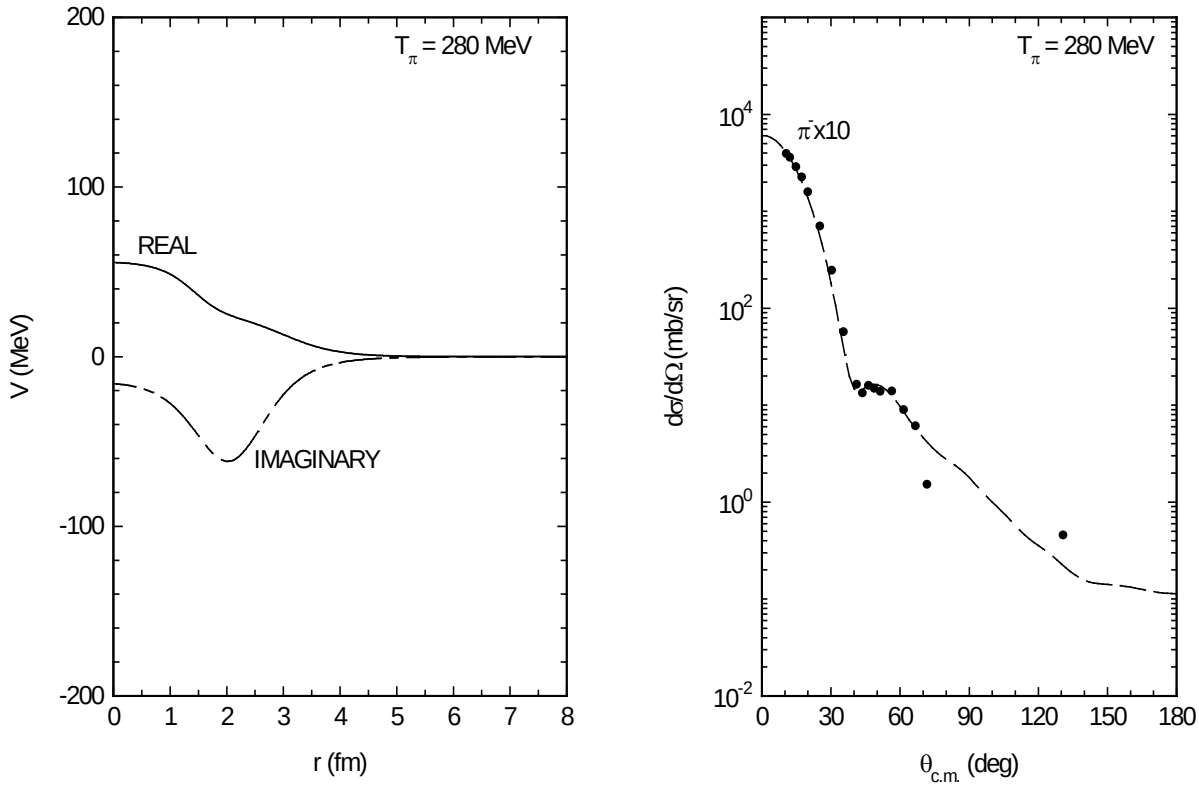

Figure 8. Same as **Figure 3** but for 280 MeV incident energy.

parts, as well as the experimental and theoretical angular distributions, are drawn in **Figure 7** and **Figure 8**. It is clear that our results support previous results indicating that the real parts of the potentials change from attractive to repulsive after 200 MeV [11] [26] [30]. On the otherhand we disagree with the theoretical results, which gave an acceptable estimate of angular distributions but not an excellent one, reported by Safari [31] indicating that the real part is repulsive even at 150 MeV for negative pions scattered from ^{12}C target.

To test the capability of our potential in accounting nicely for angular distributions and in obtaining correct reaction cross sections at higher energies *i.e.*, above the first nucleonic resonance but below the second one, we have chosen the 400 MeV case where measured elastic differential cross sections and reaction cross section are available. The potential parameters, along with reaction cross sections, are listed in **Table 1**. The potential, with its real and imaginary parts, and the calculated differential cross sections compared to the experimental ones are presented in **Figure 9**. Although the data are available only up to 60˚ in angular distribution, the fits as well as the calculated and observed reaction cross sections for π^- are in excellent agreement.

Our potential (1) used herein and for calcium target [14] [21] differ from the one proposed by Satchler who only used the first term of the real part. The addition of the second term with strength parameter V_1 is dictated by the IST extracted potential points in the exterior region. The interplay between V_o an V_1 determine the overall nature of the potential. The values of V_1 and its change from negative to positive at 230 MeV, with a small radius R_3 (approximately half the Coulomb radius R_c) and relatively small diffuseness parameter a_3, played an important role in shaping the potentials for all energies considered herein. The third and fourth terms in (1) represent, respectively, volume and surface absorptions. Since $W_3 \gg W_2$ in all but 400 MeV case, one can conclude that most of absorptions are taking place at the surface of ^{12}C, peaked around about 2.2 fm which is smaller than R_c by 0.34 fm which may be considered an approximate value of the skin depth of the ^{12}C-nucleus. This is reflected in all but the last figure. Thus, only a small fraction of pion flux reaches the interior of ^{12}C for all but the 400 MeV case. This is, of course, expected since pions will interact strongly by nucleons near the surface, and will not penetrate to the interior at least at these energies. The variation of the values of the parameters further substantiates this simple physics. In the 400 MeV case, the absorption occurs throughout the volume but the repulsive nature of the real part again allows a fraction of the flux to penetrate.

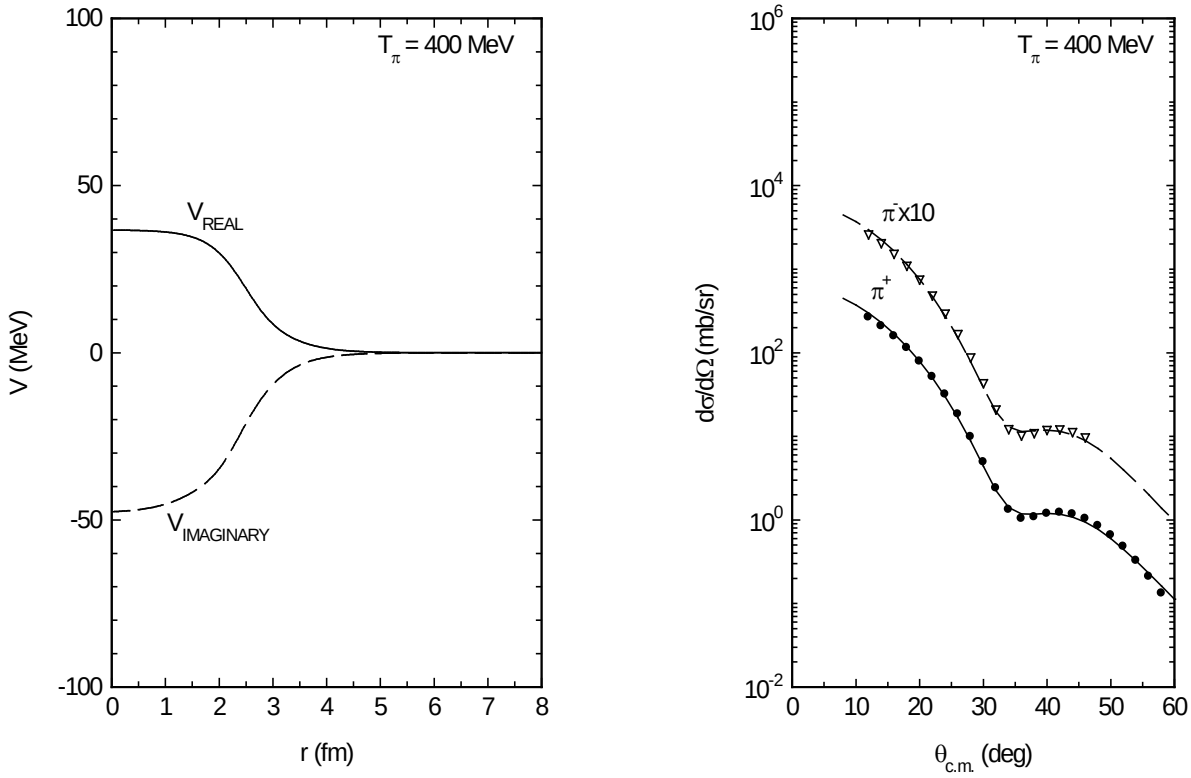

Figure 9. Same as **Figure 3** but for 400 MeV. Data are from Kahrimanis *et al.* [24].

Looking at **Table 1**, it is clear that a_o, a_1 and except for the 400 MeV, a_2 and except for the 162 and 400 MeV cases, a_3 which, in effect, determine the slope of the potential are unchanged. R_o, R_1 and R_2 are also unchanged except for the 120 and 400 MeV, 120 and 400 and 230 MeV cases, respectively. Thus in the energy range considered herein the strength parameters vary substantially. The overall strength of the real part is monotonic below the Δ–resonance but its strength reduces atop the resonance turning repulsive after the resonance, at near 230 MeV. The strength and width of W_3 which is primarily responsible for surface absorption follow roughly the variation of the magnitudes of reaction cross section with energy. The latter increases from the incident at below Δ-resonance, achieving maxima atop the resonance and then decline in its value. It seems that the effect of the Δ-resonance becomes weak around 230 MeV.

4. Conclusions

As the case for ^{40}Ca target, we demonstrate that the nuclear part of pion-^{12}C potential is the same for positive and negative pions. We establish that local optical potential in conjunction with the KG equation can suitably explain the elastic scattering as well as reaction cross sections. We further note:

a) the strength and success of IST in predicting the potential points used as a guide for constructing the correct pion-nucleus potential. This is evident here in obtaining the nature of the potential, and in particular for the time establishing the repulsive nature of the real part at 230 MeV rather definitely. Such a change in the nature of the real part was very crucial in obtaining the correct differential and reaction cross sections.

b) the simple prescription of Stricker, in substituting for Coulomb effects, is effective for a nucleus as light as ^{12}C.

c) the importance of the inclusion of $V^2(r)/2E$ term in the treatment, *i. e*. the full K-G equation, along with reliable large angle data and data on reaction cross sections in reducing the ambiguities in the parameter values that appeared in Hong *et al*.'s, Satchler's and Akhter *et al*.'s works.

d) the skin depth of the ^{12}C-nucleus is approximately 0.34 fm.

This investigation clearly establishes the importance of supplementing Satchler's potential by the second term in (1). Our potential accounts nicely for all experimental values in the whole angular range and at all energies under consideration. It also confirms that pion elastic scattering is dominated by surface absorption whose relation to pion-nucleon scattering would be important to understand.

To the best of our knowledge, all other potentials showed a limited success in giving a general description of pion elastic scattering. As such, this investigation was a timely one to rectify the remedies of previous works. In fact, it provides an important methodology to determine potentials for describing elastic scattering data for scattered charged pions from ^{12}C and other nuclei.

Acknowledgements

We acknowledge the financial support of the Deanship of Scientific Research at Taif University, Taif, Saudi Arabia for this investigation. The author also thanks Prof. F. B. Malik for fruitful discussions and his exceptional efforts in reading the revised version of the manuscript carefully.

References

[1] Lee, T.-S.H. and Redwine, R.P. (2002) *Annual Review of Nuclear and Particle Science*, **52**, 23-63. http://dx.doi.org/10.1146/annurev.nucl.52.050102.090713

[2] Morris, C.L., O'Donnell, J.M. and Zumbro, J.D. (1993) *Acta Physica Polonica B*, **24**, 1659-1671.

[3] Dytman, S.A., Amann, J.F., Barnes, P.D., *et al*. (1979) *Physical Review C*, **19**, 971-986. http://dx.doi.org/10.1103/PhysRevC.19.971

[4] Koltun, D.S. (1970) *Advances in Nuclear Physics*, **3**, Academic Press, New York, 71-191.

[5] Ericson, T. and Weise, W. (1988) Pions and Nuclei. Clarendon Press, Oxford.

[6] Kisslinger, L.S. (1955) *Physical Review*, **98**, 761-765. http://dx.doi.org/10.1103/PhysRev.98.761

[7] Fäldt, G. (1972) *Physical Review C*, **5**, 400-412. http://dx.doi.org/10.1103/PhysRevC.5.400

[8] Johnson, M.B. and Satchler, G.R. (1996) *Annals of Physics* (*New York*), **248**, 134-169. http://dx.doi.org/10.1006/aphy.1996.0054

[9] Satchler, G. (1992) *Nuclear Physical A*, **540**, 533-576. http://dx.doi.org/10.1103/PhysRevC.62.024603

[10] Khallaf, S.A. and Ebrahim, A.A. (2000) *Physical Review C*, **62**, 024603-1-8. http://dx.doi.org/10.1103/PhysRevC.62.024603

[11] Ebrahim, A.A. and Khallaf, S.A. (2005) *Acta Physica Polonica B*, **36**, 2071-2085. http://dx.doi.org/10.1556/APH.25.2006.1.3

[12] Khallaf, S.A. and Ebrahim, A.A. (2006) *FIZIKA B*, **14**, 333-348. http://dx.doi.org/10.1088/0954-3899/27/4/302

[13] Md. Akhter, S., Sultana, H.S.G. and Petersen, R. (2001) *Journal of Physics G*: *Nuclear and Particle Physics*, **27**, 755-771. http://dx.doi.org/10.1088/0954-3899/27/4/302

[14] Shehadeh, Z.F., Sabra, M. and Malik, F.B. (2003) *Condensed Matter Theories*, **18**, 339-346.

[15] Hooshyar, M.A. and Razavy, M. (1981) *Canadian Journal of Physics*, **59**, 1627-1634. http://dx.doi.org/10.1139/p81-214

[16] Alam, M.M. (1991) PhD Thesis, Department of Physics, Southern Illinois University, Illinois.

[17] Shehadeh, Z.F. (1995) PhD Thesis, Department of Physics, Southern Illinois University, Illinois.

[18] Shehadeh, Z.F. (2009) *International Journal of Modern Physics E*, **18**, 1615-1627. http://dx.doi.org/10.1142/S0218301309012823

[19] Shehadeh, Z.F., Scott, J.S. and Malik, F.B. (2011) *American Institute of Physics Journal*, **1370**, 185-191. http://dx.doi.org/10.1063/1.3638100

[20] Shehadeh, Z.F. (2013) *JAAUBAS*, **14**, 32-37. http://dx.doi.org/10.1016/j.jaubas.2013.03.003

[21] Shehadeh, Z.F. (2013) *Turkish Journal of Physics*, **37**, 190-197. http://dx.doi.org/10.3906/fiz-1207-5

[22] Stricker, K. (1979) PhD Thesis, Department of Physics, Michigan State University, Michigan.

[23] Kim, Y.J., Woo, J.K. and Hoe Cha, M. (2010) *Journal of the Korean Physical Society*, **56**, 1430-1435. http://dx.doi.org/10.3938/jkps.56.1430

[24] Kahrimanis, G., Burleson, G., Chen, C.M., *et al*. (1997) *Physical Review C*, **55**, 2533-2540. http://dx.doi.org/10.1103/PhysRevC.55.2533

[25] Ahmad, I. and Arafah, M.R. (2006) *Pramana—Journal of Physics*, **66**, 1-11.

[26] Hong, S.W. and Kim, B.T. (1999) *Journal of Physics G*: *Nuclear and Particle Physics*, **25**, 1065-1078. http://dx.doi.org/10.1088/0954-3899/25/5/310

[27] Dumbrajs, O., Frohlich, J., Klein, U. and Schlaile, H.G. (1984) *Physical Review C*, **29**, 581-591. http://dx.doi.org/10.1103/PhysRevC.29.581

[28] Harvey, C.J. (1984) PhD Thesis, Department of Physics, the University of Texas at Austin, Texas.

[29] Binon, F., Duteil, P., Garron, J.P., Gorres, J., Hugon, L., Peigneux, J.P., Schmit, C., Spighel, M. and Stroot, J.P. (1970) *Nuclear Physics B*, **17**, 168-188. http://dx.doi.org/10.1016/0550-3213(70)90408-6

[30] Lee, H.K. and McManus, H. (1971) *Nuclear Physics A*, **167**, 257-270. http://dx.doi.org/10.1016/0375-9474(71)90075-3

[31] Safari, R. (2005) *Bulgarian Journal of Physics*, **32**, 292-301.